

Relaxor properties of compositionally disordered perovskites: Ba- and Bi-substituted $\text{Pb}(\text{Zr}_{1-x}\text{Ti}_x)\text{O}_3$

George A. Samara

Sandia National Laboratories, Albuquerque, New Mexico 87185, USA

(Received 30 September 2004; revised manuscript received 11 February 2005; published 22 June 2005)

Dielectric spectroscopy, lattice structure, and thermal properties have revealed the relaxor dielectric response of Ba-substituted lead zirconate/titanate (PZT) having the composition $(\text{Pb}_{0.71}\text{Ba}_{0.29})(\text{Zr}_{0.71}\text{Ti}_{0.29})\text{O}_3$ and containing 2 at. % Bi as an additive. The relaxor behavior is attributed to the compositional disorder introduced by the substitution of Ba^{2+} at the A site and $\text{Bi}^{3+/5+}$ at the B site (and possibly A site) of the ABO_3 PZT host lattice. Analysis of the results gives clear evidence for the nucleation of polar nanodomains at a temperature much higher than the peak (T_m) in the dielectric susceptibility. These nanodomains grow in size as their correlation length increases with decreasing temperature, and ultimately their dipolar fluctuations slow down below T_m leading to the formation of the relaxor state. The influences of hydrostatic pressure on the dielectric susceptibility and the dynamics of the relaxation of the polar nanodomains were investigated and can be understood in terms of the decrease in the size of the nanodomains with pressure. The influence of dc electrical bias on the susceptibility was also investigated. Physical models of the relaxor response of this material are discussed.

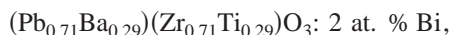
DOI: 10.1103/PhysRevB.71.224108

PACS number(s): 77.80.-e, 77.90.+k, 77.22.-d

I. INTRODUCTION

In ferroelectrics, relaxor behavior results from either frustration or compositionally induced disorder.¹ The latter type of disorder and related random fields are believed to be responsible for the relaxor properties of the most studied and most useful relaxors, the mixed ABO_3 perovskite oxides (Fig. 1).¹⁻⁹ In addition to a broad, frequency-dependent peak (T_m) in the susceptibility (or dielectric constant ϵ'), relaxors are characterized by very small remanent polarization and the absence of macroscopic phase (symmetry) change at the transition. However, there is symmetry breaking at the nanometer scale,¹ leading to the formation of polar nanodomains that exist well above T_m and strongly affect the properties. Relaxors possess very large dielectric constants, attractive for supercapacitors; exceptionally large electrostrictive coefficients, important for actuators and micropositioners; and large electrooptic constants, useful for information storage, shutters, and optical modulators. Because of these remarkable properties and their applications, relaxors are one of the most active current research areas of ferroelectricity.¹

The material studied in the present work is a mixed, hot-pressed ceramic perovskite, namely a lead/barium-zirconate/titanate with 2 at. % bismuth, an additive that increases the degree of crystalline disorder. It has the chemical composition



which henceforth will be referred to as PBZT-Bi. This material can be viewed as a chemically modified $\text{PbZr}_{1-x}\text{Ti}_x\text{O}_3$ (or PZT) as for the case of La-modified PZT (or PLZT).^{1,4,10} In the PZT system where the Zr and Ti ions are randomly distributed over the B sites of the ABO_3 lattice (Fig. 1), both FE and AFE phase transitions are observed depending on the composition. Although the presence of both Zr and Ti ions on the B sites does in principle introduce compositional dis-

order, the close similarity of the two ions in terms of their valence and polarizabilities makes it possible for PZTs to maintain their ability to achieve long-range order. In PBZT-Bi, there is a random distribution of Pb and Ba ions on the A sites as well random distribution of Zr and Ti ions on the B sites (Fig. 1). Bi can take on a valence of 3+ or 5+ and can be expected to favor the B site. However, it can also occupy the A site, and, conceivably, some of the other cations in the material can also occupy antisites. Thus PBZT-Bi site disorder and point defects, which are necessarily introduced because of the different valences of the Bi ion, can be expected to impart unto the material a degree of disorder that breaks the translational symmetry and disrupts the FE soft mode, leading to loss of correlations among of polar nanodomains resulting in relaxor behavior. We find that this is indeed the case.

We have investigated the dielectric, lattice structure and thermal properties of this PBZT-Bi material over a broad range of temperatures. Additionally the influence of hydrostatic pressure and dc biasing fields on the dielectric response

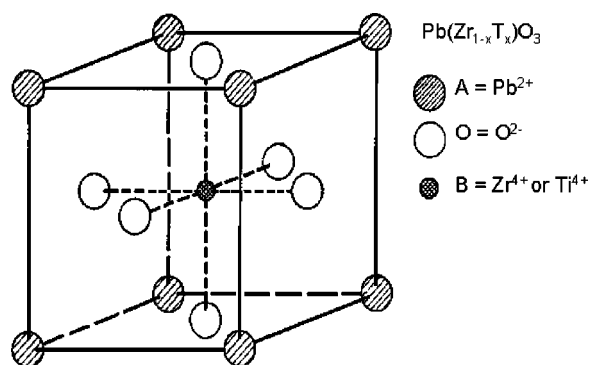


FIG. 1. The ideal cubic ABO_3 perovskite structure showing the locations and valences of the ions in PZT. In PBZT-Bi, Ba^{2+} substitutes for Pb^{2+} and $\text{Bi}^{3+/5+}$ substitutes for B^{4+} or possibly also A^{2+} sites.

were investigated. The results that are presented and discussed in what follows will provide a detailed view of the static and dynamic dielectric response and show the material to be a classic relaxor.

II. EXPERIMENTAL DETAILS

The response of a dielectric to an oscillating electric field is expressed in terms of the complex dielectric function $\epsilon = \epsilon' - i\epsilon''$. The in-phase (with the field) component of the polarization determines the real part, ϵ' , whereas the out-of-phase component determines the imaginary part, ϵ'' . ϵ'' is directly related to the dielectric loss, $\tan \delta$, which is in turn directly related to the conductivity $\sigma(\omega)$, where ω is the angular frequency of the ac field. The relationships are $\epsilon'' = \epsilon' \tan \delta = 4\pi\sigma(\omega)/\omega$.

Measurements of ϵ' and $\tan \delta$ were performed as functions of temperature, T , (77–700 K), frequency, f , (10^2 – 10^6 Hz) and hydrostatic pressure, p , (0–20 kbar). The samples were hot-pressed ceramics cut in the shape of thin plates ($\sim 0.40 \text{ cm}^2 \times 0.08 \text{ cm}$), the large faces of which were vapor coated with chromium followed by gold electrical contacts. Some of these measurements also included the influence of dc biasing fields. The pressure measurements were performed in two apparatus, one using helium and the other a mixture of normal- and isopentanes as the pressure-transmitting media. The former operates in the T range 4–400 K, and the latter in the range 290–800 K. The broad ranges of the parameters available made it possible to obtain detailed characterization of the dynamics of the relaxational response. The dielectric results were complemented by differential scanning calorimetry and x-ray diffraction measurements at 1 bar.

III. RESULTS AND DISCUSSION

A. Atmospheric pressure properties

Figure 2 shows the temperature dependences of ϵ' and ϵ'' at 1 bar measured at different frequencies. These are classic dipolar glass, or relaxor responses with strong frequency dispersion. The dispersion ultimately vanishes at sufficiently low T where all dipolar motion freezes, and the dielectric response becomes simply determined by the lattice's ionic vibrations, or infrared polarizabilities, and the electronic polarizabilities of the ions.

The very broad $\epsilon'(T)$ and $\epsilon''(T)$ peak of PBZT-Bi are other characteristic properties of a relaxor. To emphasize this feature, we superimpose on Fig. 2 a typical $\epsilon'(T)$ response of a PTZ ceramic, which exhibits a normal FE transition. Whereas the width at half max of the latter response is about 40 K, the comparable width for the PBZT-Bi sample is about 200 K.

The conclusion that the above features in the dielectric response point to the relaxor nature of PBZT-Bi is supported by the absence of a structural transition at T_m , as demonstrated by differential scanning calorimetry (DSC), differential thermal analysis (DTA), and x-ray diffraction measurements. Figure 3 shows x-ray diffraction patterns at 296 and 373 K. The patterns are identical indicating that the structure

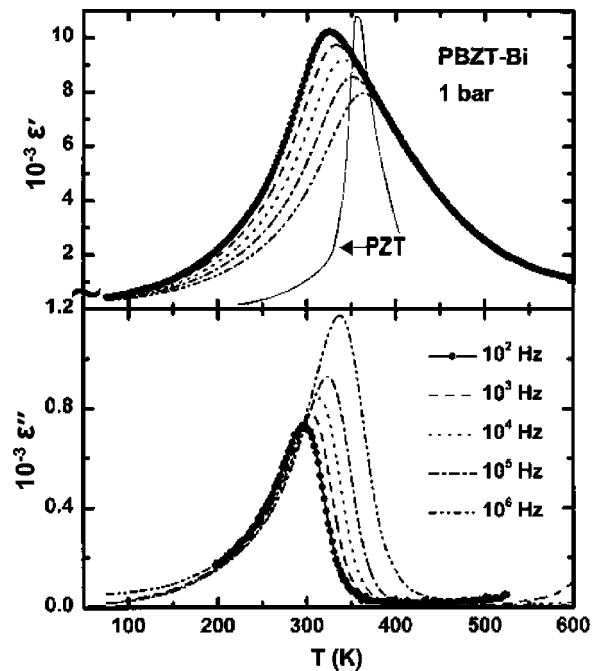


FIG. 2. Temperature dependences of the real (ϵ') and imaginary (ϵ'') parts of the dielectric constant of PBZT-Bi at 1 bar showing the strong frequency dispersion. Superimposed on the $\epsilon'(T)$ response is a typical ceramic PZT response showing a much reduced peak width.

remains cubic on going from the high T side to the low T side of the dielectric anomalies in Fig. 2. Thus, the x-ray diffraction data show that there is no *macroscopic* phase transition in PBZT-Bi in the temperature range corresponding to the observed peaks in $\epsilon'(T)$, as is expected for a relaxor. This is confirmed by the DTA scan shown in the inset in Fig. 3, where there is no indication of any endothermic or exothermic peaks on either cooling or heating.

Having established the relaxor nature of the dielectric response of PBZT-Bi, we should comment briefly about the origin of the $\epsilon'(T)$ peak. It is now well established that relaxor behavior in the ABO_3 perovskites is attributed to compositional disorder and lattice defects which break translational symmetry and long-range correlations.^{1,2} One manifestation of this disorder is the condensation of local dipolar nanodomains, or clusters, leading to local, randomly oriented polarization at a temperature (the Burns temperature, T_d)^{3,11} much higher than the peak temperature (T_m) in the $\epsilon'(T)$ response. Evidence for the existence of these nanodomains in PBZT-Bi will be presented in Sec. III B below.

Above T_d the local dipolar regions are dynamically disordered by strong thermal fluctuations. On cooling below T_d , the polar nanodomains increase in size as the polarizability of the host perovskite lattice increases, and ultimately correlations develop as the thermal disordering effects decrease. However, because of the high degree of random site disorder (which implies short correlation lengths), the correlations are weak and unable to drive the system to long-range ferroelectric order below T_m . Instead, the polar nanodomains exhibit slowing down of their polarization fluctuations, resulting in a glasslike, relaxor state with short-range order below T_m .^{1,2}

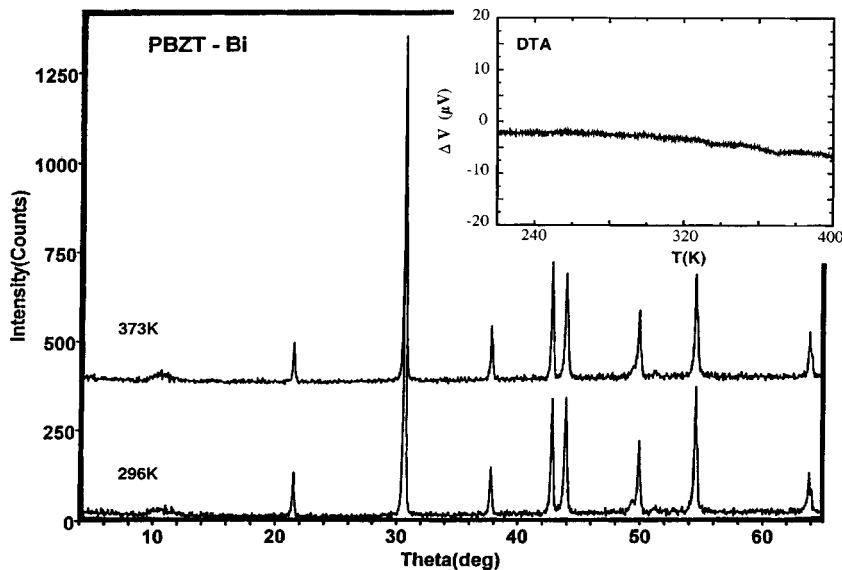


FIG. 3. X-ray diffraction patterns of PBZT-Bi at 296 and 373 K are essentially identical demonstrating the absence of a crystallographic phase transition in this temperature range. The inset shows a heating DTA scan again showing no indication of a phase transition.

The $\epsilon'(T)$ peak then reflects the competition between the developing correlations and slowing down of the dipolar fluctuations on cooling. These latter effects become dominant below T_m leading to the maximum in $\epsilon'(T)$. The relaxor state is characterized by a distribution of relaxation times that is reflected in the observed frequency dispersion in the dielectric response.

B. Evidence for the existence of polar nanodomains above T_m

There is considerable evidence that polar nanodomains exist in relaxor ferroelectrics at temperatures much higher than T_m . At these high temperatures, there is random + and - fluctuations of the polarization of these domains resulting in zero average polarization, $\Sigma P_d = 0$, i.e., there is no measurable spontaneous or remanent polarization. However, $\Sigma P_d^2 \neq 0$, and we then expect the existence of these polar domains to be manifested in properties which depend on P^2 , e.g., electrostriction and the quadratic electro-optic effect which is reflected in the refractive index, or birefringence. Indeed, both of these properties have provided quantitative measures of these polarization for a number of relaxors.^{1,2} In particular, Burns *et al.*¹¹ demonstrated the manifestation of polar nanodomains in the temperature dependence of the refractive index for several optically transparent relaxors including PLZTs. Because of lack of optical transparency, it is difficult to do electro-optic measurements on PBZT-Bi; however, thermal expansion data give clear evidence for the electrostrictive influence of polar nanodomains in this material. Evidence also comes from our high temperatures $\epsilon'(T)$ data.

In the presence of electrostriction, the thermal strain, s , for a cubic perovskite at high T is given by^{1,2}

$$s = \Delta a/a_0 = \alpha(T - T^*) + (Q_{11} + 2Q_{12})P_d^2, \quad (1)$$

where α_0 is lattice constant at the reference temperature T^* , α is the coefficient of linear thermal expansion, and the Q 's are electrostrictive constants. The normal behavior (i.e., in the absence of electrostriction) of a solid at sufficiently high T is for s to vary linearly with T , i.e., the first term on the

right-hand side of Eq. (1). Figure 4(a) shows that $s(T)$ for PBZT-Bi is highly nonlinear over the range of the measurements, but the data¹² (solid line) suggest an asymptotic approach to a linear (dashed line) response above ~ 625 K. The slope of the dashed line is $\alpha = 1 \times 10^{-5}$ K, a value common to many cubic perovskites at high T . Thus the thermal expansion of PBZT-Bi is anomalous; specifically, the rate of thermal contraction decreases continuously on cooling below ~ 625 K. This anomalous response, i.e., the additional thermal expansion denoted by the shaded region in Fig. 4(a) is

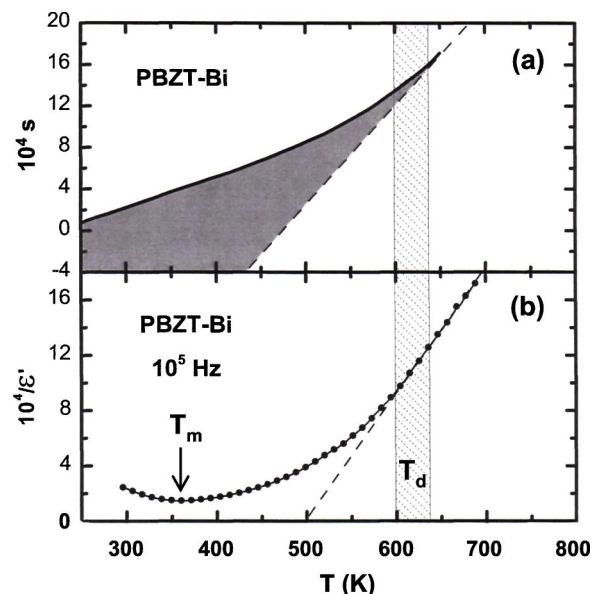


FIG. 4. (a) The linear expansion of PBZT-Bi plotted as fractional change in length, vs temperature at 1 bar. The dashed line represents the expected linear high temperature limit. Deviation from the dashed line below ~ 600 K is attributed to electrostriction. (b) Temperature dependence of $1/\epsilon'$ showing that Curie-Weiss behavior obtains only above 600 K. The shaded bar denotes the region (the Burns temperature, T_d) for the onset of polar nanodomain formation in PBZT-Bi.

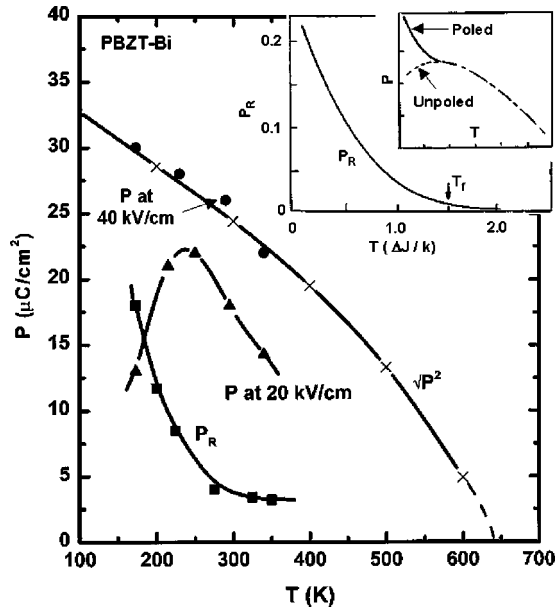


FIG. 5. Temperature dependence of the local dipolar polarization of nano-size domains ($\sqrt{P^2}$) in PBZT-Bi calculated from the anomalous thermal expansion due to electrostriction. Shown for comparison are polarization data on PBZT-Bi: specifically, the temperature dependences of the remanent polarization P_R and of the polarization at 20 and 40 kV/cm over the ranges of the available data. The inset shows the temperature dependences of the remanent polarization (P_R) and of the polarization (P) of samples initially in the poled and unpoled states of a relaxor deduced from Monte Carlo simulations (adapted from Gui *et al.* Ref. 18). T_f is the dipole freezing temperature.

due to electrostriction, or the second term on the right-hand side of Eq. (2).

The results in Fig. 4(a) would allow determination of the T dependence of P_d^2 if the values of the Q 's in Eq. (2) were known. Q_{11} and Q_{12} are not known for PBZT-Bi, but they are known for some perovskites, and we can use these to guess-timate $P_d^2(T)$ for PBZT-Bi. Assuming that the value of $(Q_{11} + 2Q_{12})$ for PBZT-Bi is comparable to the known value for PMN ($=0.39 \times 10^{-12}$ c.g.s.) yields the results in Fig. 5, plotted (solid line through the x points) as $\sqrt{P_d^2}$ vs T . Although this assumption may lead to considerable uncertainty in the absolute values of P_d^2 , it is certain that the general behavior of $\sqrt{P_d^2}(T)$ in Fig. 5 is correct. The results indicate that $\sqrt{P_d^2}$ vanishes at $T \cong 625$ K which is, of course, the temperature where deviation from linear thermal expansion set in [Fig. 4(a)]. ($T=625$ K is T_{Burns} below which nanodomains make their presence known.) Above 625 K thermal fluctuations are so large that there are no well-defined dipoles.

Figure 5 compares the calculated response of PBZT-Bi with polarization measurements at an applied field of 40 kV/cm (solid circle).⁴ The fact that the $P(T)$ data at this field nearly fall on the $\sqrt{P_d^2}(T)$ curve could be either fortuitous (given the above assumptions) or the electrostrictive constants [more specifically the quantity $(Q_{11} + 2Q_{12})$] for PBZT-Bi are comparable to those for PMN. In the latter case, the results would imply that all the polarization of the polar nanodomains in PBZT-Bi is aligned with the field at 40 kV/cm.

The polarization at 20 kV/cm in Fig. 5 falls well below $\sqrt{P^2}(T)$ and has the unusual convex shape shown. This electric field is roughly twice the coercive field, but is clearly insufficient to align all of the nanodomains at the high temperature end of the data, i.e., above ~ 250 K in Fig. 5. Cooling below 250 K, the critically slowed down polar nanodomains become harder and harder to align at 20 kV/cm, and consequently P decreases with decreasing T as shown.

Also shown in Fig. 5 is the T dependence of the remanent polarization, P_R measured at zero applied field from high (saturation) field hysteresis loops. Note that above T_m (~ 325 K in Fig. 5) P_R is relatively small ($\sim 3 \mu\text{C}/\text{cm}^2$) and nearly T independent, but below T_m it increases quite rapidly with decreasing temperature achieving a quite substantial value ($\sim 18 \mu\text{C}/\text{cm}^2$) at the lowest temperature (~ 170 K) of the data. Strictly speaking, P_R should be zero at all temperatures for a dipolar glass consisting of noninteracting dipoles or dipolar clusters. The measured finite value of P_R in Fig. 5 above T_m could be due either to some finite conductivity in the sample used or to weak correlations among the nanodomains. We believe it is the latter because the dielectric losses of the sample are very low ($\tan \delta < 0.01$). The large increase in P_R with decreasing temperature below T_m is, however, direct evidence of significant correlations (and growth in size) among the critically slowed down domains resulting in their orienting one another in the presence of the high poling field and retaining some of this orientation upon removing the field. This finding is also a manifestation of the observation that P achieves essentially full saturation at 40 kV/cm.

Evidence for the existence of polar nanodomains in PBZT-Bi above T_m also comes from the dielectric response. Whereas $\epsilon'(T)$ of a normal ferroelectric obeys the Curie-Weiss law, $\epsilon' = C/(T - T_0)$, above T_c , the $\epsilon'(T)$ response of a relaxor exhibits strong deviation from this law over a broad range of temperatures above T_m . It is now well established^{1,10} that this deviation sets in when polar nanodomains first become discernible, i.e., for $T \leq T_d$. Figure 4(b) shows that the deviation for PBZT-Bi sets in at ~ 600 K, i.e., at nearly the same T where the deviation from linear thermal expansion sets in [Fig. 4(a)]. This finding establishes this temperature as the T where polar nanodomains first form.

The $\epsilon'(T)$ response of PBZT-Bi between T_d and T_m is shown in more detail (as $1/\epsilon'$ vs T) for two frequencies in Fig. 6. The data can be fairly well fit by the generalized expression

$$\epsilon' \propto (T - T_m)^{-\gamma} \quad (2)$$

(inset Fig. 6(b)). This expression with $\gamma=2$ was thought to be a general result for relaxors;¹³ however, a closer examination of the data in Fig. 6 (see dashed line in the inset) reveals that $\gamma=2$ does not provide a very accurate fit. More generally, it has been observed¹ that no single value of γ is found which uniquely describes the $\epsilon'(T)$ dependence of relaxors. Rather different γ 's can be found for given relaxors depending on the width of the temperature window above T_m and on the frequency of the measurement.

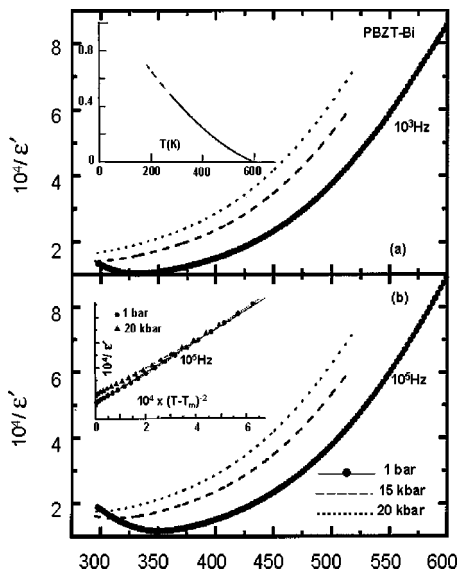


FIG. 6. Temperature dependence of $1/\epsilon'$ of PBZT-Bi at two frequencies and different pressures showing the strong deviation from Curie-Weiss behavior. The inset in (b) shows the data plotted as $1/\epsilon'$ vs $(T-T_m)^{-2}$. The inset in (a) shows the evolution of the local order parameter q on cooling.

Deviation from Curie-Weiss behavior of $\epsilon'(T)$ above T_m can be likened unto similar deviation of the T dependence of the magnetic susceptibility, χ , of spin glasses above the freezing temperature of spin fluctuations, T_f . For an ideal superparamagnet, i.e., for noninteracting paramagnetic particles or clusters, $\chi(T)$ exhibits Curie-Weiss behavior. This behavior is achieved in spin glasses for temperatures $\gg T_f$. At lower temperatures deviation from the Curie-Weiss law is attributed to strong local magnetic correlations^{1,10} and the onset of local (spin-glass) order below T_f . Sherrington and Kirkpatrick¹⁴ developed a model, which relates $\chi(T)$ below T_f to the local order parameter q . The expression is

$$\chi = \frac{C[1 - q(T)]}{T - T_0[1 - q(T)]}, \quad (3)$$

where it is seen that q is a function of temperature. Clearly q and its temperature dependence can be evaluated from $\chi(T)$ data and the values of C and T_0 determined from the high temperature $\chi(T)$ response above T_f which follows a Curie-Weiss law. In this high temperature limit $q \rightarrow 0$ and Eq. (3) simply reduces a Curie-Weiss form. Equation (3) can be thought of as a modified Curie-Weiss law, where both C and T_0 are functions of temperature.

If we presume, as we believe to be the case, that the deviation from Curie-Weiss behavior in PBZT and other relaxors is due to correlations among local polar nanodomains, then we can invoke for $\epsilon'(T)$ an expression similar to that in Eq. (3), where the local order parameter due to correlation between neighboring polar regions of polarizations P_j and P_j is $q \equiv \langle P_j P_j \rangle^{1/2}$. Such an expression has been shown to provide a satisfactory description of the $\epsilon'(T)$ response of the relaxor PMN,¹⁰ and we find it to be also satisfactory for PBZT-Bi. We have used the data in Figs. 4(a) and 6 to cal-

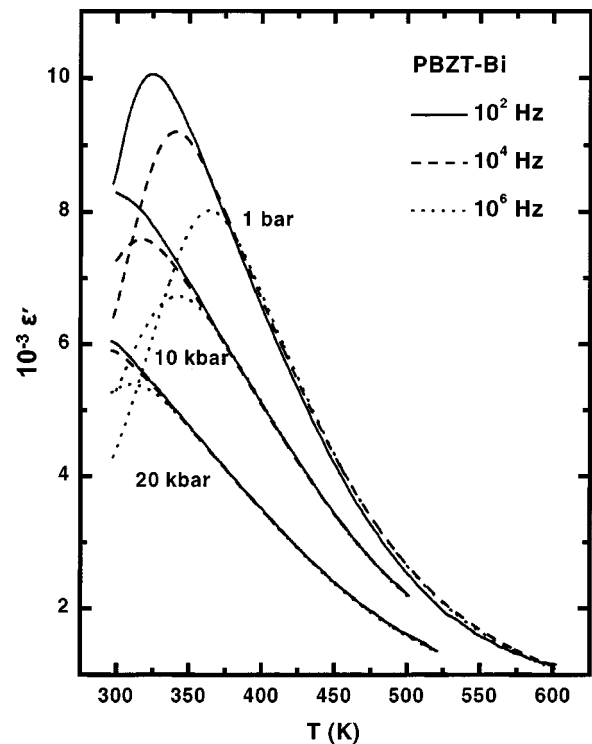


FIG. 7. Temperature and pressure dependences of the dielectric constant (ϵ') of PBZT-Bi measured at different frequencies and pressures above ambient temperature.

culate the temperature dependence of q . The results are shown in the inset in Fig. 6(a). As expected, $q \rightarrow 0$ at ~ 600 K and increases with decreasing temperature below 600 K because of increased correlations.

C. Effects of pressure and dc bias

Hydrostatic pressure suppresses T_m , ϵ' , and $\tan \delta$ of PBZT-Bi. Some results are shown in Figs. 6 and 7. These pressure effects are manifestations of the influence of pressure on the soft mode frequency of the host lattice.^{1,15} This frequency is determined by a delicate balance between short-range and long-range (Coulomb) forces, and these forces exhibit markedly different dependences on interatomic separations, or pressure. Specifically, pressure increases the soft mode frequency at constant temperature, which reduces the polarizability of the PZT host lattice, thereby reducing the correlation length for dipolar interactions and correlations among nanodomains.^{1,15} The result is a shift of T_m to lower temperatures and a suppression of the $\epsilon'(T)$ response. Figure 8 shows the pressure dependence of T_m at different frequencies. The responses are linear over the pressure range covered, the slopes $d T_m / d P$ varying from -2.6 K/kbar at 10^2 Hz to -2.9 K/kbar at 10^6 Hz indicating a weak decrease in the frequency dispersion of T_m with pressure. Figure 6 shows that although pressure has a significant influence on the magnitude of $\epsilon'(T)$, the functional form of $\epsilon'(T)$ remains essentially unchanged.

The application of a dc biasing electric field can provide useful information about the kinetics and energetics of do-

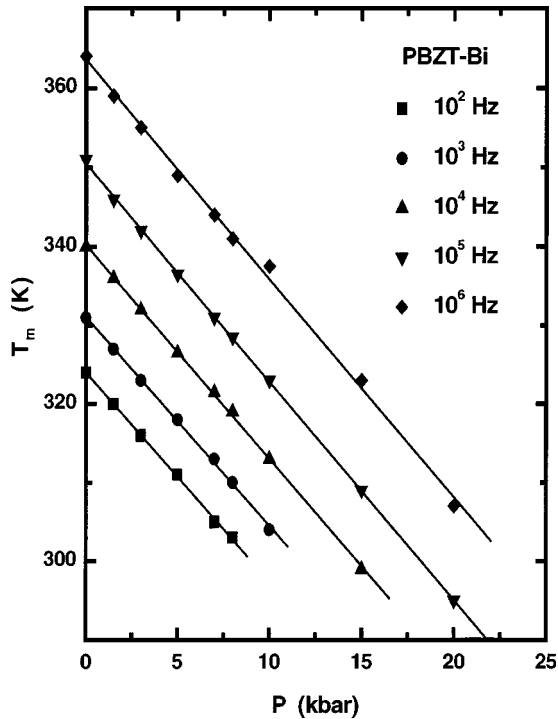


FIG. 8. Pressure dependences of the dynamic glass transition temperature (T_m) of PBZT-Bi showing the frequency dispersion in T_m which corresponds to the peak in $\epsilon'(T)$.

main reorientation in relaxors. We have therefore investigated the effects of dc bias on the dielectric response of PBZT-Bi. A bias field of 5 kV/cm has essentially no effect on the $\epsilon'(T)$ response in Fig. 2. This is not surprising in view of the high fields (~ 40 kV/cm) required to align domains and achieve saturation of the polarization. A 5 kV/cm field is simply not enough to align domains, especially below T_m where it is more energetically difficult to do so (see Fig. 5). Fields in the 10–15 kV/cm range cause 25%–40% suppression in the amplitude of the $\epsilon'(T)$ peak,¹² an effect attributed largely to the alignment of some domains thereby clamping the small signal ac polarizability.

In relaxors that are close in chemical composition to the normal FE-to-relaxor crossover, the application of a dc bias can often transform a relaxor to ferroelectric for sufficiently large fields. We have seen such effects, for example, in studies of La-modified PZTs (or PLZTs).^{1,15} The field enhances the growth of macroscopic polar domains on lowering the temperature, resulting in the FE state. For PBZT-Bi fields on the order of 40 kV/cm are needed to induce such a transition.

D. Dynamics of dipolar freezing

Figure 9 shows a more detailed view of the relaxational dielectric response. These results, which are highly reproducible and reflect the high quality of the material, provide a detailed view of the dynamics of the dipolar freezing process. They define relaxation frequencies, f , corresponding to the peak temperatures, T_m , and characteristic relaxation times, $\tau=1/\omega$, where $\omega=2\pi f$ is the angular frequency.

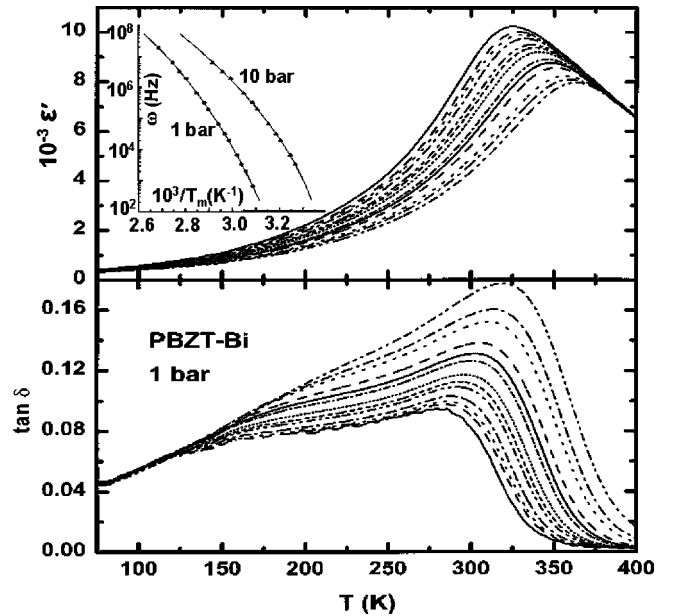


FIG. 9. Temperature dependences of the dielectric constant (ϵ') and dielectric loss ($\tan \delta$) of PBZT-Bi measured at 1 bar and different frequencies (10^2 – 10^6 from left to right) providing a detailed view of the dynamics of the dipolar freezing process. The inset shows the non-Arrhenius character of the relaxation frequency at 1 bar and 10 kbar.

Since relaxation processes are usually thermally activated, it is natural to present relaxation data as Arrhenius plots of $\ln \omega$ vs $1/T_m$. Such plots for the present data at 1 bar and at the higher pressures reveal the non-Arrhenius character of the response as shown in the inset in Fig. 9 and has also been observed for other relaxors.¹ This departure from Arrhenius behavior can be satisfactorily described (solid lines) by the Vogel-Fulcher (V-F) equation

$$\tau^{-1} = \omega = \omega_0 \exp[-E/k(T_m - T_0)], \quad (4)$$

which is found to be applicable to many relaxational phenomena.¹ E is the energy barrier between equivalent dipole directions, and T_0 is a reference temperature where all relaxation times diverge (and where the distribution of τ 's becomes infinitely broad). The PBZT-Bi data can be fit by this expression; however, it is difficult to obtain a unique fit over a relatively small range of frequency. Reasonable fitting parameters are $E=0.17(0.15)$ eV, $T_0=250(230)$ K, and $\omega_0=10.0(4.4) \times 10^{13}$ Hz for the 1 bar (10 kbar) data, respectively. The decrease in E is a manifestation of the decrease in the size of the polar nanodomains with pressure, as will be discussed later. Simply stated, E is proportional to the volume and smaller domains are easier to reorient than larger domains, hence, a lower E . The decrease in T_0 with pressure is the expected response for a perovskite.¹ It is satisfying to note that the V-F fit yields a value of dT_0/dp that is very comparable to the observed shifts of the dynamic glass transition temperature, T_m , in Fig. 8.

E. Physical model for the relaxor behavior of PBZT-Bi

The relaxor behavior of PBZT-Bi is undoubtedly brought about by the substitutions of Ba^{2+} and $\text{Bi}^{3+}/\text{Bi}^{5+}$ ions into the parent PZT lattice. These ions, with sizes, polarizabilities and valences (in the case of Bi) different from those of the host lattice, introduce lattice disorder (including oxygen vacancies and off-center positions) that breaks the translational symmetry and long-range order leading to the relaxor state. The situation here is somewhat akin to that in the more studied La-substituted PZTs, or PLZTs.^{1,10} For these latter relaxors, it has been pointed out that T_d , coincides with the FE transition temperature, T_c , of the parent PZT having the same Zr/Ti ratio.¹¹ We find that this is also true for PBZT-Bi where T_d (Fig. 4) is essentially T_c (=610 K) of $\text{PbZr}_{0.71}\text{Ti}_{0.29}\text{O}_3$ (PZT 71/29). Equating T_d with T_c of the host PZT highlights the physical meaning of T_d , namely the temperature where polar nanodomains become discernible.

For PBZT-Bi, as for PLZT, one can picture the formation of two types of local order below T_d . In one, groups of unit cells (clusters) exist that do not contain substituent ions and thus retain the character of the parent PZT, forming ordered polar nanodomains. The high degree of compositional disorder, which breaks the translational symmetry, keeps these nanodomains small, and prevents them from forming a long-range-ordered, normal FE state. For the relatively high concentrations of Ba and Bi in our present sample, we do not expect many clusters of this type. In the second type, dipolar entities introduced by substituents polarize small regions around them in the highly polarizable host also forming randomly oriented polar nanodomains. These nanodomains grow in size with decreasing T as the polarizability of the host lattice, and thereby the correlation length, r_c , for dipolar interactions (which is inversely proportional to the FE soft mode frequency, ω_s)¹ increases (Fig. 10). However, here again the high degree of compositional disorder prevents the formation of a FE state, and ultimately slowing down of the dipolar fluctuations sets in at $T \leq T_m$ for both types of domains, leading to the formation of a relaxor state.

The decrease of T_m and the suppression of the dielectric anomaly with pressure (Figs. 7 and 8) are characteristics of ABO_3 relaxors and can be understood in terms of soft mode theory.¹ Specifically, pressure stiffens ω_s , reducing r_c and leading to the observed effects in Figs. 7 and 8. Figure 10 shows the large influence of pressure on r_c for PBZT-Bi. Thus, e.g., at 350 K, r_c decreases by 30% in 20 kbar, and thereby the decrease in correlation volume (=size of nanodomain) is very large. These results were obtained from the dielectric data, since $r_c \propto \sqrt{\epsilon'}$. (This simply comes from the fact that $r_c \propto 1/\omega_s$, the soft mode frequency, and $\omega_s^2 \epsilon' = \text{constant}$.) This procedure yields relative, not absolute, values of r_c , and, thus, r_c in Fig. 10 is given in arbitrary units.

F. Model theories

Since relaxors are materials with random site lattice disorder, it is natural to resort to models that investigate the role of random fields. In the ABO_3 relaxors the polar nanodomains create random electric fields in the host lattices. The lattice strains, x_{ij} , associated with these domains also

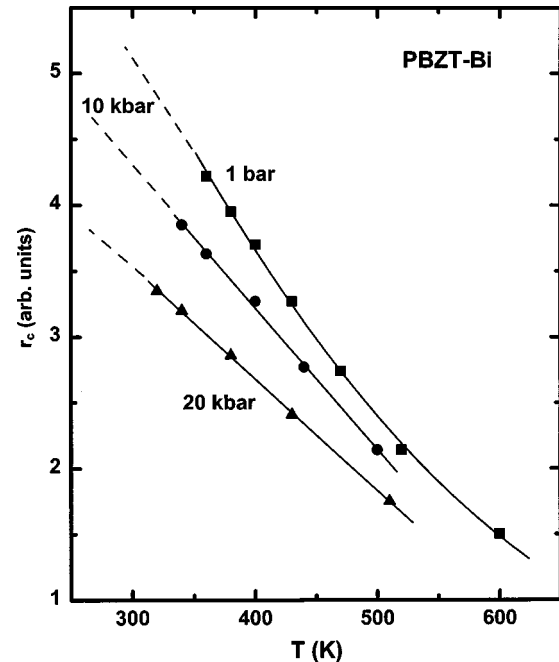


FIG. 10. Effects of temperature and pressure on the correlation length, r_c , for dipolar interactions in PBZT-Bi.

couple to the polarization via terms of the $x_{ij}P_kP_l$ setting up additional random fields or enhancing their presence. The simplest approach to treating the physics has been to employ an Ising pseudospin model in random field.¹⁶ While this model provides a qualitative picture, it has serious deficiencies in treating the relaxor problem. Since the basic reorientable polar nanodomains, or “pseudospins,” vary in both size and orientation, relaxors cannot be described by an ordering field of fixed length. This issue was one of the main motivations for the development of the spherical random bond/random field model for relaxors.¹⁷ This model has been shown to provide a reasonable description of the properties of several ABO_3 relaxors, including PLZTs and the pressure dependence of their phase behavior.^{15–17} It should be applicable to PBZT-Bi as well.

Considering PBZT-Bi to be made up of ordered (or polar) nanoregions embedded in a disordered matrix, it is possible to simulate its polarization response using a Monte Carlo approach. The material can be pictured as consisting of Ising-like dipoles on a regular lattice with randomly distributed exchange energy parameters.

Using this approach Gui *et al.*¹⁸ simulated a $16 \times 16 \times 16$ simple cubic lattice with periodic boundary conditions. The inset in Fig. 5 shows the calculated temperature dependence of the remnant polarization, P_R , where temperature is in units of $(\Delta J/k)$. Freezing of dipoles occurs at $T_f = 1.5\Delta J/k$, where J is an effective exchange energy and k is Boltzmann’s constant. Note the collapse of P_R near the dipole freezing temperature, T_f , and the close qualitative similarity of these results to the experimental data on PBZT-Bi in Fig. 5. The inset in Fig. 5 also shows the simulated change of the polarization with increasing temperature under the influence of a dc-biasing field ($E=0.6\Delta J/\bar{\mu}$) for samples initially in the poled and unpoled states ($\bar{\mu}$ is the maximum projec-

tion of the dipole moment on the main axis). These simulated results also manifest the main features of the experimental results on PBZT-Bi shown in Fig. 5. Specifically, for PBZT-Bi an external field of 20 kV/cm is not sufficient to reorient the polarization at low temperatures, and thus $P(T)$ exhibits a maximum, as shown in Fig. 5. This corresponds to the unpoled case in the inset. On the other hand, if we were to saturate the polarization of PBZT-Bi at low temperatures, e.g., as obtains for the 40 kV/cm data in Fig. 5, and then lower the bias field to something less than a saturation field, say 20 kV/cm, and then heat, we would expect behavior similar to that for the poled case in the inset in Fig. 5. Specifically, very rapid decrease in P with increasing temperature at low temperatures because a 20 kV/cm field is not able to keep the domains aligned at these temperatures. At a sufficiently high temperature, corresponding to the peak in the inset, the poled and unpoled responses are expected to merge. Thus, the model is capable of qualitatively reproducing the $P(T, E)$ results on PBZT-Bi.

IV. SUMMARY AND CONCLUDING REMARKS

The results presented show that the PBZT-Bi composition investigated exhibits classic relaxor behavior. The dielectric responses are akin to those of PLZTs with sufficiently high

La content.¹ In both systems the relaxor state results from the high degree of compositionally induced lattice disorder that breaks down dipolar correlations effectively reducing the observed pressure-induced ferroelectric-to-relaxor crossover in a wide variety of compositionally disordered perovskites, demonstrating that the relaxor state is the ground state of these materials under pressure (or at reduced volume).¹⁵ Consistent with this view, we have shown in the present work that r_c of PBZT-Bi is strongly reduced by pressure, effectively resulting in smaller nanodomains and strengthening the glasslike character of the response. The observed decrease in the activation energy for dipole reorientation supports this view.

ACKNOWLEDGMENTS

The author expresses strong appreciation to Donald Overmyer for the x-ray measurements, Terry Aselage for differential scanning calorimetry measurements, and Leonard Hansen for experimental support. The work was supported in part by the Division of Materials Sciences and Engineering, Office of Basic Energy Sciences, U.S. Department of Energy (DOE). Sandia is a multiprogram laboratory operated by Sandia Corporation, a Lockheed Martin Company, for the U.S. Department of Energy under Contract No. DE-AC04-94AL85000.

-
- ¹G. A. Samara, in *Solid State Physics*, edited by H. Ehrenreich and F. Spaepen (Academic, New York, 2001). Vol. 56, pp. 239–483 and reference therein.
- ²E. Cross, *Ferroelectrics* **76**, 241 (1987).
- ³M. L. Mulvihill, S. E. Park, G. Risch, Z. Li, K. Uchino, and T. R. ShROUT, *J. Appl. Phys.* **35**, 3984 (1996).
- ⁴D. Viehland, M. Wuttig, and L. E. Cross, *Ferroelectrics* **120**, 71 (1991); *Phys. Rev. B* **46**, 8003 (1993), and references therein.
- ⁵Z. G. Ye and H. Schmid, *Ferroelectrics* **145**, 83 (1993).
- ⁶V. Westphal, W. Kleemann, and M. D. Glinchuk, *Phys. Rev. Lett.* **68**, 847 (1992).
- ⁷E. V. Colla, N. K. Yushin, and D. Viehland, *J. Appl. Phys.* **83**, 3298 (1998).
- ⁸V. Bobnar, Z. Kutnjak, R. Pirc, and A. Levstik, *Phys. Rev. B* **60**, 6420 (1999).
- ⁹C. Ang, Z. Yu, J. Hemberger, P. Lunkenheimer, and A. Loidl,

- Phys. Rev. B* **59**, 6665 (1999).
- ¹⁰X. Dai, A. DiGiovanni, and D. Viehland, *J. Appl. Phys.* **74**, 3399 (1993); *Philos. Mag. B* **70**, 33 (1994), and reference therein.
- ¹¹G. Burns and F. H. Dacol, *Phys. Rev. B* **28**, 2527 (1983), and reference therein.
- ¹²From earlier Sandia measurements.
- ¹³K. Uchino, S. Nomura, L. E. Cross, S. J. Jang, and R. E. Newnham, *J. Appl. Phys.* **51**, 1142 (1980).
- ¹⁴D. Sherrington and S. Kirckpatrick, *Phys. Rev. Lett.* **35**, 1972 (1975).
- ¹⁵G. A. Samara, *Ferroelectrics* **274**, 183 (2002).
- ¹⁶See, e.g., B. E. Vugmeister, *Ferroelectrics* **120**, 133 (1991).
- ¹⁷R. Pirc and R. Blinc, *Phys. Rev. B* **60**, 13470 (1999); *AIP Conf. Proc.* **535**, 30 (2000).
- ¹⁸H. Gui, B. Gu, and X. Zhang, *Ferroelectrics* **197**, 63 (1997).